Journal of Radioanalytical and Nuclear Chemistry (2023) 332:423–434
https://doi.org/10.1007/s10967-023-08773-z

Simultaneous correction of the coincidence summing and self-absorption for radioactivity measurement in solid samples by MCNP-CP code

Le Quang Vuong[1,2] · **Tran Thien Thanh**[1,2,3] · **Phan Long Ho**[1,2,4] · **Le Cong Hao**[1,2,3] · **Chau Van Tao**[1,2,3]

Received: 14 October 2022 / Accepted: 6 January 2023 / Published online: 14 January 2023

Abstract
The present work of this study involves an advanced analytical procedure that allows direct and fast determining the specific activity of ^{238}U and ^{235}U using the gamma-rays of 63.3 keV and 185.7 keV after subtraction of the contribution of overlapping peaks. This procedure also included MCNP-CP code in order to calculate the coincidence summing and the self-absorption correction factor. Validation of the developed procedure was confirmed by the IAEA proficiency test to calculate the activities of radionuclides in various types of samples such as rich thorium, secular equilibrium, and disequilibrium of uranium. The final scores were received "acceptable" for all radionuclides.

Keywords Gamma spectrometry · MCNP-CP · Overlapping peak · Self-absorption · Direct method · Proficiency test

Introduction

Measuring uranium is important in many studies such as the monitoring and warning of nuclear activity [1], the evaluation of the radiological naturally occurring radioactive material concentrations and the impact on workers and public members [2], the interpretation of the luminescence dating of sediment [3, 4], the assessment of radioactivity to prevent public health risks [5–7]. The activity of uranium isotopes and their decay daughters can be determined by inductively coupled plasma mass spectrometry [8], alpha spectrometry [9, 10], and liquid scintillation counting [11]. However, these methods require lengthy and complicated destructive techniques for the samples with an unknown chemical matrix which make the whole process inconvenient and costly.

Gamma spectrometry is a widely used non-destructive measurement technique for the determination of radioactive materials in environmental samples. Its advantages are not requiring laborious sample preparation whilst providing information of various radionuclides at the same time. ^{238}U activity concentration is indirectly calculated based on the activities of ^{214}Pb and ^{214}Bi if the secular equilibrium exists in the analysis sample [12, 13]. In addition, ^{234}Th is the nearest daughter of ^{238}U and has a short half-life (24.10 ± 0.03 days [14]) compared to ^{238}U (4.468 ± 0.005 billion years). This can lead to the secular equilibrium between ^{238}U and ^{234}Th in the soil, rock, and sediment samples if the effect of geochemical processes is ignored [15]. Therefore, the direct measurement of the 63.3 keV peak emissions can give simultaneous information on ^{234}Th and its parent ^{238}U in the sample [16, 17]. On the gamma-ray spectra, the energy region of 63 keV is overlapped by three gamma-rays including the 63.3 keV peak emitted from ^{234}Th ($3.75 \pm 0.08\%$ emission probability), 63.9 keV peak emitted from ^{231}Th ($0.0235 \pm 0.0021\%$), and 63.8 keV peak emitted from ^{232}Th ($0.259 \pm 0.015\%$). The nuclide ^{231}Th is the nearest daughter of ^{235}U. Because natural uranium comprises a small proportion of ^{235}U (0.72% of natural uranium) and the emission probability of the 63.9 keV gamma-ray (^{231}Th) is lower than the 63.3 keV (^{234}Th) and 63.8 keVgamma-rays (^{232}Th), the interference of ^{231}Th at the 63 keV region can be neglected. However, the contribution of ^{232}Th leads to

---

✉ Tran Thien Thanh
ttthanh@hcmus.edu.vn

[1] Department of Nuclear Physics, Faculty of Physics and Engineering Physics, University of Science, Ho Chi Minh City, Vietnam

[2] Vietnam National University, Ho Chi Minh City, Vietnam

[3] Nuclear Technique Laboratory, University of Science, Ho Chi Minh City, Vietnam

[4] Institute of Public Health in Ho Chi Minh City, Ho Chi Minh City, Vietnam

the remarkably large systematic influence of 0.8–122% in the measured ^{238}U activity via the gamma-ray 63.3 keV of ^{234}Th [18]. Besides, the self-absorption correction (C_{abs}) is also a large uncertainty associated with ^{234}Th measurements at the peak of 63.3 keV.

These C_{abs} factors of samples with 3.3 mm thickness are approximately 4% for moss soil (IAEA-447), 15% for phosphogypsum (IAEA-434) [19], on the contrary, it is 8% for a Marinelli beaker geometry with about 0.5 litter volume of soil [20], and 7–20% for phosphate rocks thickness varying from 10 to 50 mm [21]. Therefore, a reliable analysis of ^{238}U activity according to the 63.3 keV peak requires taking into account the accurate corrections for the self-absorption effect as well as the contribution of ^{232}Th at the 63 keV region.

Natural uranium consists of three main radioactive isotopes ^{238}U (99.2745% abundance), ^{235}U (0.72%), and ^{234}U (0.0055%). The ^{235}U analysis from the peak of 143.8 keV (0.94 ± 0.06% emission probability), 163.4 keV (5.08 ± 0.03%), and 205.3 keV (5.02 ± 0.03%) energy transitions is impossible because the counting rates due to these peaks are often below the detection limits of the HPGe p-type detector. For that reason, the activity concentration of ^{235}U is generally determined from the peak of 185.7 keV (57.0 ± 0.3% emission probability) after the subtracting of ^{226}Ra contribution at 186.2 keV (3.56 ± 0.02%) [22, 23]. The determination of ^{226}Ra by gamma spectrometry has been based on the detection of emissions of its daughter nuclides ^{214}Pb and ^{214}Bi in the secular equilibrium [24–26]. The disadvantages of this method are that it requires a long waiting time to ensure the secular equilibrium of ^{226}Ra—its progeny (at least a month) and it requires the calculation of the coincidence summing correction factor for gamma-rays emitted from ^{214}Pb or ^{214}Bi, which can lead to a relative deviation of 40% for the measured ^{238}U activity concentration [27].

In this work, a rapid and reliable analytical procedure is applied to determine the activity concentration of ^{238}U and ^{235}U using the gamma-rays of 63.3 keV emitted from ^{234}Th and 185.7 keV emitted from ^{235}U. This procedure is focused on the careful consideration of the detection efficiency, the self-absorption correction, the coincidence summing correction, and the contributions of ^{232}Th and ^{226}Ra for the energy region of 63 keV and 186 keV, respectively. Its advantage is it may be applied immediately after the sample preparation regardless of the existence of a secular equilibrium between ^{226}Ra and its progenies (^{214}Pb, ^{214}Bi) and regardless of the existence of equilibrium between ^{238}U and ^{226}Ra or normal ^{235}U-^{238}U isotopic ratio. The certified reference material (CRM) samples with varying amounts of uranium and thorium are measured for the calculation of the activity concentration of ^{238}U and ^{235}U by using the advanced analytical procedure. The results of radioactivities are evaluated in the IAEA proficiency test.

Theory

Monte Carlo simulation

Monte Carlo simulation with MCNP-CP upgrade patch version 3.2 was a powerful and reliable tool for the simulation of modeling real source responses and efficiencies of the detector. It was developed to upgrade the standard MCNP version 6 software. The properties of a decay scheme of a particular radionuclide were considered from the evaluated nuclear structure data file [28]. CPS card (Correlated Particle Source) was used to perform the statistical simulation of processes accompanying the radioactive decay of a specified radionuclide, yielding correlated characteristics of emitted particles, and tracked within the same history. The model simulation of detector, lead shield, and the sample container was described in a similar way to the experimental system.

The element concentrations taken from Table 1 were used for the simulations. Two simulated responses were obtained

Table 1 The information of the samples

Sample	Dry mass (g)	Density (g cm^{-3})	The concentration of element (%)												
			O	Na	Mg	Al	Si	P	S	K	Ca	Ti	Fe	Sr	Zr
Reference															
RGU	130	1.55	53.0	–	–	0.3	46.4	–	–	0.1	–	–	0.2	–	–
IAEA-434	76	0.91	58.0	0.8	0.2	–	1.6	1.6	15.3	0.1	22.3	–	0.1	–	–
IAEA-447	108	1.29	65.3	0.5	0.5	3.7	11.6	–	0.2	1.4	12.6	0.2	4.0	–	–
RGTh	119	1.42	52.9	0.2	0.2	0.3	45.5	0.2	–	0.1	0.2	–	0.2	0.1	0.1
Rock															
S1	145	1.74	56.4	–	0.1	3.2	37.4	–	–	1.5	0.1	0.2	0.3	–	0.8
S2	144	1.72	57.2	–	–	2.6	38.2	–	–	1.1	0.1	0.1	0.2	–	0.5
S3	152	1.81	58.2	0.1	0.1	2.9	36.6	–	–	0.9	0.1	0.1	0.5	–	0.5
S4	138	1.65	60.0	–	0.1	4.2	34.4	–	–	–	0.2	0.1	0.7	–	0.3
S5	118	1.40	62.5	–	0.1	10.4	22.3	–	–	1.5	–	0.8	2.2	–	0.2

for each radionuclide emitting cascade gamma-rays. The first output file was defined with an uncorrelated source, which can be obtained by tracking each gamma-ray in separate history (FEP efficiency "without—ε_{wo}(E)"). The second output file showed that the result corresponded to the case of total correlation between all the particles emitted, which were tracked within the same historical (FEP efficiency "with—ε_{w}(E)"). The relative uncertainty was adjusted to be less than 0.01% with the 10^9 number particles of 10^9 historical simulations. The coincidence summing correction factor (CSF) for gamma-rays emitted from radionuclides in the ^{235}U, ^{238}U, and ^{232}Th series was calculated by the equation:

$$CSF = \frac{\varepsilon_{wo}(\mathrm{E})}{\varepsilon_{w}(\mathrm{E})} \tag{1}$$

The material samples were placed in a cylindrical container of the same geometric scale, but they were composed of entirely different materials. Therefore, the self-absorption correction factor (C_{abs}) was required to account for differences in attenuation coefficients for the samples as follows [29]:

$$C_{abs} = \frac{\mu_2(\mathrm{E})}{\mu_1(\mathrm{E})} \times \frac{1 - \exp(-\mu_1(\mathrm{E}) \times x)}{1 - \exp(-\mu_2(\mathrm{E}) \times \mathrm{x})}. \tag{2}$$

where $x = 2\,cm$ is the thickness of the samples, $\mu_1(E)$ and $\mu_2(E)$ are the linear attenuation coefficients (cm^{-1}) for energy E of the RGU standard and the analysis samples, respectively.

We considered three approaches for determining the self-absorption correction factor at the 63.3 keV peak, including:

- *First method* the total attenuation of the sample, μ_ρ(E) (cm^2 g^{-1}), was taken from the XCOM database [30] and calculated the linear attenuation coefficient by formula $\mu = \mu_\rho(\mathrm{E}) \times \rho$, where $\rho\,(g\,cm^{-3})$ was density. The self-absorption correction factor was determined by using Eq. (2).
- *Second method* the gamma spectra of MCNP-CP simulation was used to calculate the linear attenuation coefficient. The input file of MCNP-CP code was performed using the densities of samples from 0.2 to 2.2 (g cm^{-3}) with an increment of 0.2 (g cm^{-3}), the samples thicknesses from 0.2 to 3.0 cm with 0.2 cm increment. According to the method from Huy et al. [31], the effective attenuation coefficient μ_{eff} (cm^{-1}) can be calculated from two fitting curves. The first curve was an exponential function for the relationship between the simulation FEP efficiencies and the sample densities. As the result, the effective attenuation coefficient was calculated with each thickness of the sample and a mass attenuation coefficient can be expressed by formula $a = \mu_{eff}/\rho$, where $a\,(cm^2\,g^{-1})$. The second fitting curve was a quadratic polynomial function that illustrated the relationship between the mass attenuation coefficients and the samples thickness. Finally, the self-absorption correction factor was determined by using Eq. (2).
- *Third method* the self-absorption correction factor can be obtained as the ratio of the FEP efficiencies between the standard sample ($\varepsilon_0(E)$) and the analytical sample ($\varepsilon(E)$) from the same sample-detector geometry (Eq. (3)), which were simulated by MCNP-CP code with an uncorrelated source:

$$C_{abs} = \frac{\varepsilon_0(E)}{\varepsilon(E)}. \tag{3}$$

Experimental

Gamma spectrometric measurements are done using the coaxial p-type HPGe detector (supplied by ORTEC, GEM50P4-83 model) with a crystal diameter of 65.9 mm, crystal length of 77.0 mm, and relative efficiency of 50% [32]. The energy resolution (FWHM) at 122 keV (^{57}Co) and 1332 keV (^{60}Co) are 0.9 keV and 1.9 keV, respectively. The detector is shielded by a cylindrical low-background lead with different thicknesses of low-carbon steel, lead, tin, and copper layers of 13 mm, 101 mm, 0.5 mm, and 1.6 mm, from outside to inside, respectively. The gamma spectra are acquired 16,384 channels to record photon energy up to 3000 keV by Maestro software [33]. The analysis of spectrometric data is performed by Colegram software [34] aimed at obtaining the best results for the peaks of interest.

The RGU standard and the CRM samples, needed to validate the advanced analytical procedure, were supplied by the International Atomic Energy Agency (IAEA). Five rock samples (labeled from S1 to S5) were collected in Southern Vietnam. All samples were prepared by grinding to powder, then drying the powder at 105 ± 10 °C to a constant weight. They were sieved using a 200 µm sieve, then the powder obtained was homogenized. Each sample was split. One part was used to analyze radionuclides. The powder was packed in a cylindrical polyethylene container with an external diameter of 75 mm, an external height of 47 mm, a wall thickness of 1 mm, and was pressed to a thickness of 20 mm. This process had been applied to handle geological samples and has proven reliable to get radon (^{222}Rn, had an approximate half-life of 3.82 days) not escape from the container [25]. The sample containers were positioned on the detector endcap, aligned with the detector axis. Acquisition time ranged from 86 400 to 172 800 s for the gamma spectra of the background and samples.

The analytical procedure to determine direct radioactivity in solid samples is presented in Fig. 1. The heavy metals in samples were analyzed by the X-ray fluorescence

Fig. 1 Overview of the advance analytical procedure applied to determine directly the activity concentration of ^{238}U and ^{235}U by gamma spectrometry

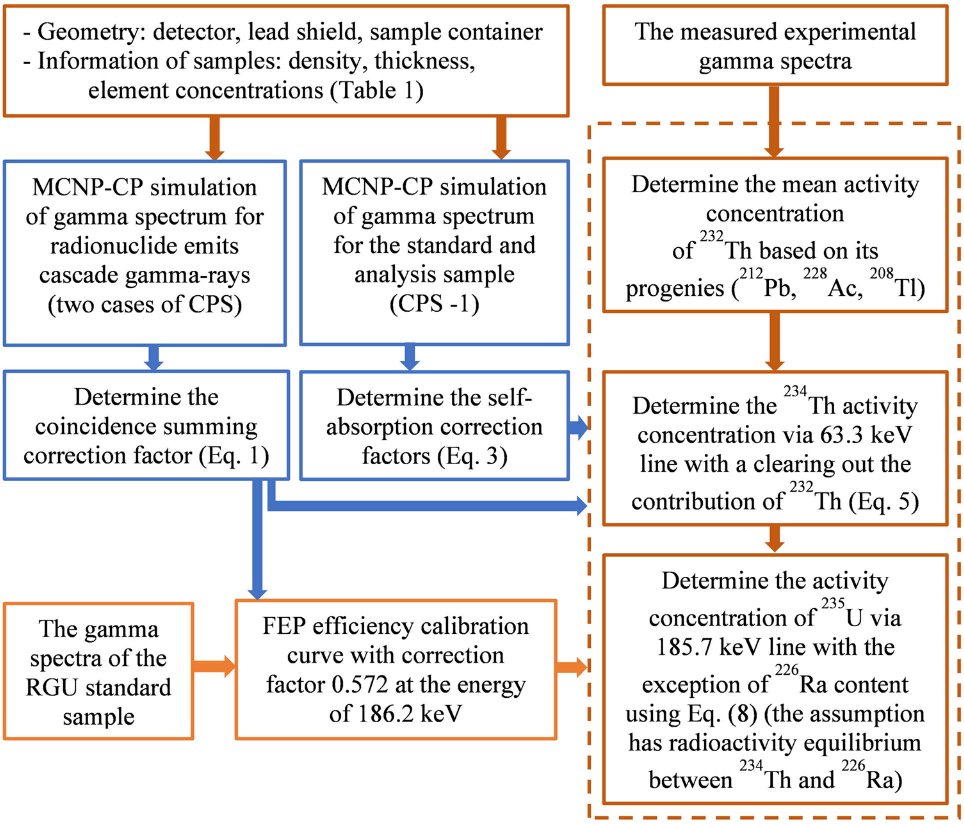

system (model S2-Puma, [35]). Oxygen concentration was calculated by excluding the total of other elements. The element concentration results to be used for the correction of self-absorption for each sample are presented in Table 1.

Calculations

The activity concentration of radionuclide for each peak with energy E is calculated by the following formula:

$$A_i = \frac{N_P(E_i)}{I_\gamma(E_i) \times \varepsilon_P(E_i) \times m \times t} \Pi C_i, \quad (4)$$

where A_i, m, t, $N_P(E_i)$, $I_\gamma(E_i)$, $\varepsilon_P(E_i)$ are the activity concentration (Bq kg^{-1}), the dry mass (kg), the acquisition live time (s), the net peak areas, the emission probability of separate gamma-rays, the FEP efficiency, respectively. ΠC_i is the product of different correction factors such as the coincidence summing effect, self-absorption effect, etc.

Because the total counts of the 63 keV region includes the contribution counts of ^{232}Th (63.8 keV, 0.26 ± 0.02% emission probability) and ^{234}Th (63.3 keV, 3.75 ± 0.08%), the counts at the peak 63.3 keV (^{234}Th) can be calculated by using the formula:

$$N^{63.3}_{^{234}Th} = N^{63}_{total} - N^{63.8}_{^{232}Th} = N^{63}_{total} - \frac{A_{^{232}Th} \times \varepsilon_{63.8} \times I^{63.8}_{^{232}Th} \times m \times t}{\Pi C_i^{63.8}}. \quad (5)$$

The activity concentration of ^{232}Th ($A_{^{232}Th}$) is calculated based on the mean activity of respective progenies such as ^{228}Ac (338.3, 911.2 and 969.0 keV), ^{212}Pb (238.6 keV), and ^{208}Tl (583.2 keV), using the following formula:

$$\overline{A} = \frac{\sum_{i=1}^{n} \frac{A_i}{u_i^2}}{\sum_{i=1}^{n} \frac{1}{u_i^2}}, \quad (6)$$

$$\overline{u} = \frac{1}{\sqrt{\sum_{i=1}^{n} \frac{1}{u_i^2}}}. \quad (7)$$

where n is the number of isotopes, A_i and u_i are the activity concentration and absolute uncertainty of ith isotopes, respectively.

Similarly, the counts of the 186 keV region includes the contribution counts of ^{235}U (185.7 keV, 57.0 ± 0.3% emission probability) and ^{226}Ra (186.2 keV, 3.56 ± 0.02%). The contribution of ^{235}U at the 186 keV energy region can be calculated by the formula:

$$N^{185.7}_{^{235}U} = N^{186}_{total} - \frac{A_{^{226}Ra} \times I^{186.2}_{^{226}Ra} \times \varepsilon_{186.2} \times m \times t}{\Pi C_i^{186.2}}. \quad (8)$$

The half-life of ^{226}Ra is very small compared with ^{238}U (1600 years compared with 4.468 billion years, respectively). When the sampling area has not undergone recent geochemical changes and there are no natural disturbances of the decay series, the secular equilibrium can exist between ^{238}U and its progenies (^{234}Th, ^{226}Ra, ^{214}Pb, ^{214}Bi). The present work considers three options for the evaluation of ^{226}Ra content including the calculated activity of ^{226}Ra based on the direct measurement of ^{234}Th 63.3 keV line (First option), using the correction factor of 57.2% ^{226}Ra at the 186 keV region (Second option), and the calculating mean activity of ^{226}Ra based on its daughters (^{214}Pb and ^{214}Bi) (Third option). The ^{235}U specific activity will be determined by using Eq. (4) and Eq. (8).

Minimum detectable activity (MDA) is an important parameter in low-level activity measurements using the gamma spectrometry. It depends on the detector efficiency for photon energy, emission probability, acquisition time, etc. In the case of peaked backgrounds, the MDA for each energy of radionuclide is calculated by the formula [36]:

$$\mathrm{MDA} = \mathrm{w} \times \frac{k^2 + 2k\sqrt{B + B\frac{N}{2n}}}{1 - (k \times \sigma_{\mathrm{w}})^2}. \quad (9)$$

where N is the number of channels in the peak region, B is the background number of counts in N channels, n is the number of channels at the left and right of the ROIs, $\mathrm{w} = \frac{1}{\varepsilon_P(E_i) \times I_\gamma(E_i) \times m \times t}$, σ_{w} is the fractional uncertainty of w. The coverage factor used is $k = 1.645$. The count number of the background is calculated by interpolating the continuous background under the peak from the adjacent regions in a gamma-ray spectrum. The ROIs used for calculating B is four times the FWHM and adds two channels to the left and two channels to the right of an expected centroid. According to the law of uncertainty propagation, MDA's relative uncertainty is evaluated.

Results and discussion

Validation of MCNP-CP calculating the coincidence summing and self-absorption corrections

The reliability of MCNP-CP code for calculating coincidence summing correction factor (CSF) in gamma spectrometry considering volume source has been performed by the testing equivalence of computer codes [32, 37]. In this study, the CSF for ^{235}U, ^{234}Th, ^{226}Ra, ^{214}Pb, ^{214}Bi, ^{228}Ac, ^{212}Pb, and ^{208}Tl were determined by MCNP-CP simulation (Supplementary data). The CSF results were ranging from 0.97 to 1.21 and presented a good agreement with the results from Ordóñez et al. [38].

Figure 2 illustrates the self-absorption correction factors for 63.3 keV gamma-ray which were calculated by all three methods with the range of 0.93 to 1.08. These results were compared to the correction factors from Thanh et al. [19] and showed a good agreement with the maximum relative deviation of 5.8% and 3.2% for IAEA-434 and IAEA-447 samples, respectively. Table 2 presented the statistical pairwise comparison of the self-absorption correction factors at the peak of 63.3 keV (234Th) for the samples including IAEA-434, IAEA-447, RGTh, and S1-S5 samples. The contrast means the differences in the comparison of the different methods. The result of the contrast was -0.0038 showing that the self-absorption correction factor at the peak of 63.3 keV with the second method was lower than the first method by 0.0038 with a 95% confidence interval -0.0623 to 0.0548. In contrast, the self-absorption correction factor of the third method was higher than that of the first and second methods by 0.0038 and 0.0075, respectively. This confirms that the self-absorption correction factor calculated by the third method was reliable to apply to the measurement of gamma-emitting radionuclides in solid samples. There were several explanations including:

- The first method was simple and quick to estimate the self-absorption factor for the analytical sample. However, it was based on the assumption of a parallel photon beam

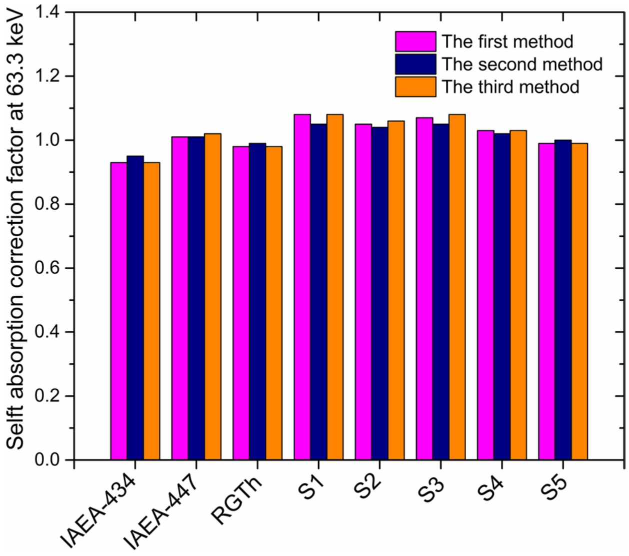

Fig. 2 The self-absorption correction factor at the peak of 63.3 keV (^{234}Th) for the samples

Table 2 The pairwise comparisons of the results of the self-absorption correction factor at the peak of 63.3 keV (^{234}Th) for the samples

The pairwise comparisons	Pairwise comparisons of means of the self-absorption correction factor		
	Contrast	Standard error	[95% Confidence interval]
2nd method versus 1st method	− 0.0038	0.0232	[− 0.0623–0.0548]
3rd method versus 1st method	0.0038	0.0232	[− 0.0548–0.0623]
3rd method versus 2nd method	0.0075	0.0232	[− 0.0511–0.0661]

in Eq. (2), which was not fulfilled in the applied close measurement geometry. In fact, the radiations originating from the side of the sample near the detector would be less likely to be attenuated than the radiations from deep within the sample, which must pass through the material of the sample to reach the detector.

- The second method confirmed the reliability of the Monte Carlo calculation for the self-absorption factor of the 63.3 keV gamma-ray. However, this method required a large amount of data from the simulation, which was used to fit with the mathematical functions.
- Regarding the third method, the self-absorption correction factor was determined by the ratio of FEP efficiency between the standard sample and the analytical sample that was calculated by the MCNP-CP simulations in the same close measurement geometry. Therefore, it depended only on the sample thickness, density and chemical composition and not on geometry effects [31, 39].

Impact of the 186.2 keV peak on the experimental full energy peak efficiency calibration curve

The RGU sample (activity concentration 4940 ± 30 Bq kg^{-1}) was used to establish the calibration FEP efficiency curve for the HPGe detector in the energy range from 46.5 to 2447.9 keV. The experimental efficiencies were determined at the sixteen energies of gamma-rays which were emitted from radionuclides such as ^{210}Pb (46.5 keV), ^{234}Th (63.3 and 92.5 keV), ^{226}Ra (186.2 keV), ^{214}Pb (242.0, 295.2, and 351.9 keV) and ^{214}Bi (609.3, 768.4, 934.1, 1120.3, 1238.1, 1281.0, 1764.5, 2204.2, and 2447.9 keV). The CSF of these radionuclides was calculated by MCNP-CP code. The relative uncertainty of experimental efficiency for the ^{234}Th doublet gamma emission at 92.5 keV (total emission probability 4.33 ± 0.38%) was 8.8%, which corresponded to the combined standard uncertainties (k = 1) [40]. This doublet was the mean energy of 92.4 keV (2.18 ± 0.19%) and 92.8 keV (2.15 ± 0.19%) energy transitions from ^{234}Th decay. Moreover, several researchers have noted that thorium has $K_{\alpha 1}$ X-ray at 93.3 keV, which will overlap at 92.5 keV, so it is very difficult to correct for analyzing ^{234}Th at this energy on the gamma spectrum [41]. The relative uncertainties of the experimental efficiencies for the other gamma-ray energies were less than 2.5%. Two cases were applied to investigate the results of the calibration FEP efficiency curves (Fig. 3), given by:

Case I using fifteen values of the experimental efficiencies for radionuclides ^{210}Pb, ^{234}Th, ^{214}Pb, ^{214}Bi, and without experimental efficiency at the peak of 186.2 keV (^{226}Ra).

Case II using sixteen values of the experimental efficiency for radionuclides. The correction factor of 0.572 was used to correct the count of ^{226}Ra at the peak of 186.2 keV [25].

Each case of FEP efficiency was fitted with a log–log polynomial by using the ACORES software [42]. Single way ANOVA [43] with the in-significant value for Bartlett's statistic (0.994) proved a statistically insignificant difference among the three group means. The result showed that the significance level (p-value) was 0.9917, which was over 0.05. In other words, there were no discriminants among FEP efficiencies (Table 3).

Figure 3 illustrates the sixteen values of the experimental efficiencies and case I of the FEP efficiency curve and case II of the FEP efficiency curve. At energies 46.5 keV, 63.3 keV, 186.2 keV, the relative deviations between the

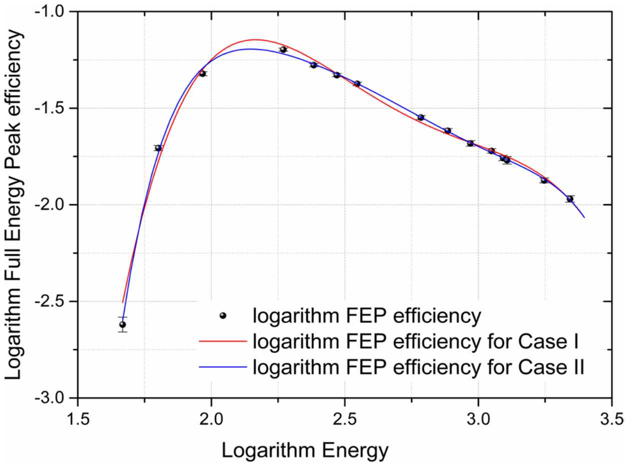

Fig. 3 Calibration of full energy peak efficiency curves using the RGU standard

Table 3 Analysis of ANOVA presents the homogeneity of variances

Group	Summary of FEP efficiency		
	Mean	Standard deviation (%)	Frequency
Experimental FEP efficiency	0.02713	0.01742	16
Case I of FEP efficiency	0.02666	0.01774	16
Case II of FEP efficiency	0.02746	0.01790	16

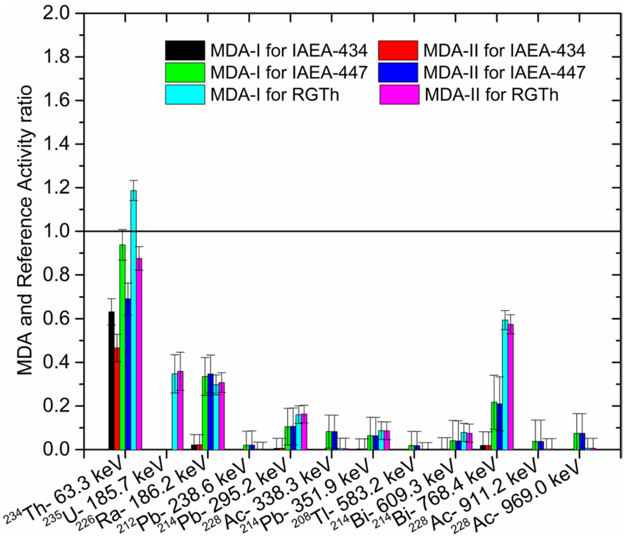

Fig. 4 Comparison of the minimum detectable activity with the reference activity for the IAEA-434, IAEA-447, and RGTh samples

experimental value and the interpolated value from the case I curve are – 23.2%, 16.7%, – 6.3%, respectively, and the relative deviations between the experimental value and the interpolated value from the case II curve are – 4.7%, 5.3%, 5.3%, respectively. These lead to the efficiency values at the 46.5 keV, 63.3 keV, and 186.2 keV peak interpolated from the case I and case II of FEP efficiencies curves having the relative deviation of 10.5%, 35.6%, and 3.3%, respectively. It showed that the FEP efficiency value at 186.2 keV energy strongly affected the calibration FEP efficiency curve for the HPGe detector.

Figure 4 shows the ratio of MDA results and reference activity for CRM samples. The MDA-II value of ^{234}Th (63.3 keV) in the RGTh sample is compared with the MDA-I value, with an improvement of 35.6%, and is lower than the certified reference activity. In addition, the MDA-II for ^{226}Ra (186.2 keV) for S1-S5 samples had a range from 3.42 ± 0.4 (Bq kg^{-1}) to 6.23 ± 0.5 (Bq kg^{-1}) and they were lower than the calculated MDA results by liquid scintillation counting [44], and by alpha spectrometry [45].

Confirmation of the analytical procedure using certified reference materials

In this work, the samples of the certified reference materials IAEA-434, IAEA-447, and RGTh were used to confirm the analytical procedure. According to Eq. (4), the activity concentration of radionuclides for the ^{232}Th, ^{238}U, and ^{235}U series were derived from the net peak areas, the photon emission probability, the calibration FEP efficiency curves of both cases (Case I and Case II), the self-absorption factor and coincidence summing correction factor. Relative bias (RB) between the measured and certified activity was determined by the formula:

$$RB(\%)=\frac{\left|\mathrm{A}_{\mathrm{measured}}-\mathrm{A}_{certified}\right|}{\mathrm{A}_{certified}}\times 100. \tag{10}$$

The IAEA assesses the proficiency test procedure in terms of both accuracy and precision. The accuracy-test compared the relative bias to the maximum acceptable relative bias (MARB) which had a range from 15 to 30% for gamma-ray emitting radionuclides [46]. For all radionuclides in this study, the MARB value was set at 15%. If RB > MARB, the accuracy-test marked the value as "Not accepted". Precision-test was applied if the measured value satisfied the accuracy-test (RB ≤ MARB): $\mathrm{RB} \le \mathrm{k} \times \mathrm{P}$ and $\mathrm{P} \le \mathrm{MARB}$. The coverage factor k = 2.58 with a probability of confidence level of 99%. The precision-test (P) was calculated by the equation:

$$P(\%)=\sqrt{\left(\frac{u_{A_{measured}}}{A_{measured}}\right)^2+\left(\frac{u_{A_{certified}}}{A_{certified}}\right)^2}\times 100. \tag{11}$$

where, $A_{\mathrm{certified}}$ and $A_{measured}$ were the certified value from IAEA and the measured value of activity concentration, respectively; $u_{A_{\mathrm{certified}}}$ and $u_{A_{measured}}$ were the corresponding standard uncertainties (k = 1), respectively. When both accuracy-test and precision-test achieved "Accepted", the final score for all analytical determinations of the proficiency tests was "Accepted". Conversely, if the accuracy was "Accepted" but the precision was "Not Accepted", the final score was "Warning".

Figure 5 illustrates the activity ratio between the measured results and the certified values of ^{232}Th and ^{238}U for the various types of reference material such as rich thorium (RGTh), secular equilibrium (IAEA-447), and disequilibrium of uranium (IAEA-434). The activity concentration of ^{226}Ra, ^{214}Pb, ^{214}Bi in the ^{238}U chain and ^{228}Ac, ^{212}Pb, ^{208}Tl in the ^{232}Th chain are higher than the MDA values and receive "Accepted" for the final scores. For the ^{234}Th activity concentration in the IAEA-447, RGTh, IAEA-434 samples, the results of measured radioactivity compared with the certified values have a relative bias of 34.3%, 127.0%, 35.7%, and

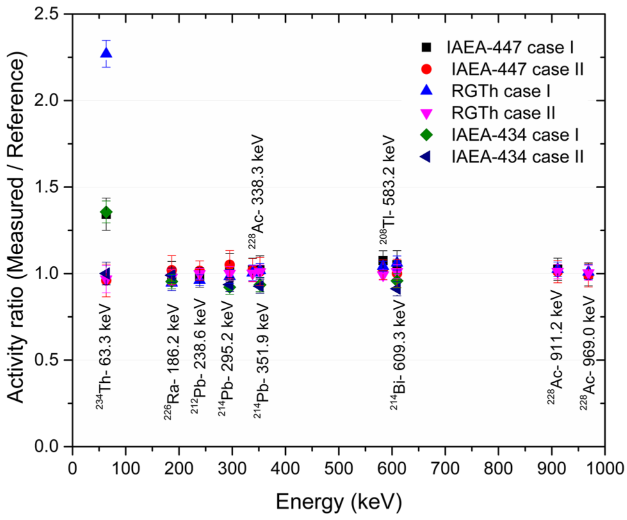

Fig. 5 Activity ratio between the measured results and the certified values of ^{238}U and ^{232}Th for the IAEA-434, IAEA-447, and RGTh samples

4.0%, 3.2%, 0.1% with the case I and case II of FEP efficiency curves, respectively (Table 4). It shows the accuracy of the measured ^{234}Th activity using the 63.3 keV gamma ray depends on the FEP efficiency, the self-absorption and the interference correction factors. The final score for the activity concentration of ^{234}Th with case II of the FEP efficiency curve is “Accepted”. This verifies that the FEP efficiency curve for case II is reliable and can be applied for measuring the radioactivities in the enviromental sample.

The p-type HPGe detector with the low energy resolution can not deconvolute the 186 keV area, the counts of both 185.7 keV (^{235}U) and 186.2 keV (^{226}Ra) are shown as a total count of 186 keV region in the gamma-ray spectrum. Therefore, to rapidly and accurately determine the ^{235}U activity concentration in environmental samples, the correction factor for the contribution of ^{226}Ra was needed (Eq. (8)). In this work, we developed an analytical process that was used to calculate the ^{226}Ra activity concentration based on the direct measurement of ^{234}Th 63.3 keV line (Eq. (5)) (called the first option). This option required a precise efficiency calibration curve, the self-absorption correction factor and the assumption has radioactivity equilibrium between ^{238}U and ^{226}Ra. Its advantage is it may be applied immediately after sample preparation as it does not rely on the equilibrium of the ^{226}Ra daughters. The second option assumed the proportions of the count rates at the 186 keV region for ^{226}Ra and ^{235}U were 57.2% and 42.8%, respectively [25], which relies on two equilibrium assumptions of the ^{238}U–^{226}Ra daughters and the natural ratio of ^{235}U–^{238}U. So this procedure will give misleading results if the measurements on samples from places where the chemical or isotopic composition has been altered. The third option relied on the secular equilibrium of ^{226}Ra and its daughters (^{214}Pb and ^{214}Bi). This technique is widely used in many environmental laboratories to determine the ^{226}Ra content, but it requires complicated sample preparation and a waiting period (about thirty days). Table 5 shows the ^{235}U activity concentration in the RGTh sample which was calculated by the direct method (first and second options) and the equilibrium method (third option). Although the results for ^{235}U with the second and third options have the status “Accepted”, their assumptions need special consideration for each type of environmental sample. Regarding the calculation of ^{235}U using the reference to the ^{234}Th activity (the direct method), the result with the case II of FEP efficiency curve is compared with the reference value, with a relative bias of less than 3%, and the final score shows “Accepted”. It confirmed that an advanced analytical procedure which was detailed in Fig. 1 can be applied to determine the ^{235}U activity in the solid sample by using the gamma spectrometry.

Determination of the radioactivities for the rock samples

The activity concentrations of radionuclides in the rock samples were determined by using the developed analytical procedure. The activity concentration of ^{232}Th had a range from 11.4 ± 0.2 (Bq kg^{-1}) to 77.7 ± 0.8 (Bq kg^{-1}), while the activity concentration of ^{238}U had a range from 9.5 ± 0.2 (Bq kg^{-1}) to 41.1 ± 0.4 (Bq kg^{-1}). These results were in agreement with the reported data for samples of various rocks collected in many countries such as China [47], Saudi Arabia [48], Egypt [49], India [50], Poland [51], and Iran [52] (Table 6).

Figure 6 shows the activity concentrations of ^{234}Th (Fig. 6a) and ^{235}U (Fig. 6b) for the rock samples, which are higher than the MDA values. A t-distribution with the two-tailed probability value (p-value) for the null hypothesis [53] is used to compare the measured activity for ^{234}Th with the ^{226}Ra mean value (^{214}Bi, ^{214}Pb). This statistical analysis is a reliable assessment method and has been validated by several studies such as Daoushy and F. Hernández [16], Ordóñez et al. [38], Vesterbacka et al. [54], and Giubrone et al. [55]. The relative deviations less than 2% and the p-value over 0.05 for the t-test statistical analysis prove no statistical difference in the activity concentration of ^{234}Th and the mean of ^{226}Ra value. For the activity concentration of ^{235}U, the results clearly indicate that a good agreement between the analytical procedure using the reference to ^{234}Th activity and the ^{235}U mean of activity with a relative deviation of less than 3%. Moreover, the specific activity ratio of uranium isotopic (^{235}U/^{238}U) is also calculated and ranges from 0.046 to 0.051. It turned out that there are no uranium ratio anomalies in the samples [56].

Table 4 Measured activities of ^{232}Th and ^{238}U series for the CRM samples

Sample	Chain	Radionuclides	Energy (keV)	Certified value (Bq kg^{-1})	Case I of FEP efficiency curve			Case II of FEP efficiency curve		
					MDA (Bq kg^{-1})	Measured activity (Bq kg^{-1})	Final score	MDA (Bq kg^{-1})	Measured activity (Bq kg^{-1})	Final score
IAEA-434	^{238}U	^{234}Th	63.3	120 ± 6	75.84 ± 2.57	163 ± 6	N	55.93 ± 2.10	120 ± 5	A
		^{226}Ra	186.2	780 ± 31	16.82 ± 0.42	744 ± 10	A	17.39 ± 0.43	773 ± 10	A
		^{214}Pb	295.2		4.47 ± 0.10	719 ± 6	A	4.55 ± 0.10	730 ± 6	A
			351.9		2.65 ± 0.06	729 ± 6	A	2.63 ± 0.06	723 ± 6	A
		^{214}Bi	609.3		2.03 ± 0.07	748 ± 7	A	1.94 ± 0.07	712 ± 7	A
		^{238}U mean value			731 ± 4	A		722 ± 4	A	
IAEA-447	^{232}Th	^{212}Pb	238.6	37 ± 2	0.75 ± 0.03	36.2 ± 0.6	A	0.78 ± 0.03	37.6 ± 0.6	A
		^{208}Tl	583.2		0.70 ± 0.03	39.8 ± 0.6	A	0.66 ± 0.02	37.8 ± 0.6	A
		^{228}Ac	338.3		3.05 ± 0.16	37.8 ± 1.5	A	3.04 ± 0.16	37.7 ± 1.5	A
			911.2		1.39 ± 0.11	37.9 ± 1.3	A	1.37 ± 0.11	37.4 ± 1.3	A
			969.0		2.78 ± 0.20	36.8 ± 1.4	A	2.76 ± 0.20	36.6 ± 1.4	A
		^{232}Th mean value			37.8 ± 0.4	A		37.6 ± 0.4	A	
	^{238}U	^{234}Th	63.3	22.2 ± 0.8	20.82 ± 1.26	29.8 ± 2.6	N	15.35 ± 0.97	21.3 ± 1.9	A
		^{226}Ra	186.2	25 ± 2	8.39 ± 0.28	24.7 ± 0.7	A	8.67 ± 0.29	25.5 ± 0.7	A
		^{214}Pb	295.2		2.62 ± 0.07	25.9 ± 0.4	A	2.66 ± 0.07	26.3 ± 0.5	A
			351.9		1.60 ± 0.04	25.5 ± 0.4	A	1.58 ± 0.04	25.3 ± 0.4	A
		^{214}Bi	609.3		1.03 ± 0.05	26.3 ± 0.4	A	0.98 ± 0.05	25.0 ± 0.4	A
		^{238}U mean value			25.8 ± 0.2	A		25.5 ± 0.23	A	
RGTh	^{232}Th	^{212}Pb	238.6	3250 ± 90	5.19 ± 0.09	3124 ± 44	A	5.39 ± 0.09	3246 ± 45	A
		^{208}Tl	583.2		3.84 ± 0.05	3387 ± 30	A	3.66 ± 0.05	3223 ± 29	A
		^{228}Ac	338.3		8.11 ± 0.31	3263 ± 117	A	8.00 ± 0.31	3254 ± 117	A
			911.2		19.13 ± 0.69	3332 ± 105	A	19.02 ± 0.69	3288 ± 104	A
			969.0			3281 ± 106	A		3262 ± 106	A
		^{232}Th mean value			3304 ± 23	A		3235 ± 23	A	
	^{238}U	^{234}Th	63.3	78 ± 3	92.59 ± 2.36	177 ± 12	N	68.28 ± 2.61	76 ± 5	A
		^{226}Ra	186.2		23.18 ± 0.57	74 ± 2	A	23.97 ± 0.56	76 ± 2	A
		^{214}Pb	295.2		12.50 ± 0.16	77 ± 1	A	12.71 ± 0.16	78 ± 1	A
			351.9		6.79 ± 0.09	79 ± 1	A	6.73 ± 0.09	79 ± 1	A
		^{214}Bi	609.3		6.14 ± 0.10	83 ± 1	A	5.84 ± 0.10	79 ± 1	A
		^{238}U mean value			80 ± 1	A		79 ± 1	A	

where A is “Accepted”, N is “Not Accepted”

Table 5 The activity concentration of ^{235}U for the RGTh sample

Analytical procedure	Certified value (Bq kg^{-1})	Case I of FEP efficiency curve			Case II of FEP efficiency curve		
		MDA (Bq kg^{-1})	Measured activity (Bq kg^{-1})	Final score	MDA (Bq kg^{-1})	Measured activity (Bq kg^{-1})	Final score
1st option	3.6 ± 0.3	1.25 ± 0.03	–	–	1.29 ± 0.03	3.7 ± 0.3	A
2nd option			3.5 ± 0.1	A		3.6 ± 0.1	A
3rd option			3.1 ± 0.1	A		3.5 ± 0.1	A

where A is “Accepted”, N is “Not Accepted”

Table 6 Comparison of activity concentration of ^{238}U and ^{232}Th series for rock samples in the present study to the other researches

Research	Activity concentration (Bq kg^{-1})	
	^{232}Th	^{238}U
Present work	11.4–77.7	9.5–41.1
Lu et al. [47]	19.9–53.6	10.7–34.8
Trabulsy et al. [48]	5.3–58.9	5.2–29.3
Harb et al. [49]	7.5–171	3.4–212
Rangaswamy et al. [50]	52.5–117.9	22.1–59.8
Dżaluk et al. [51]	2.4–71.6	5.2–52.6
Dżaluk et al. [52]	2.4–71.6	5.2–52.6

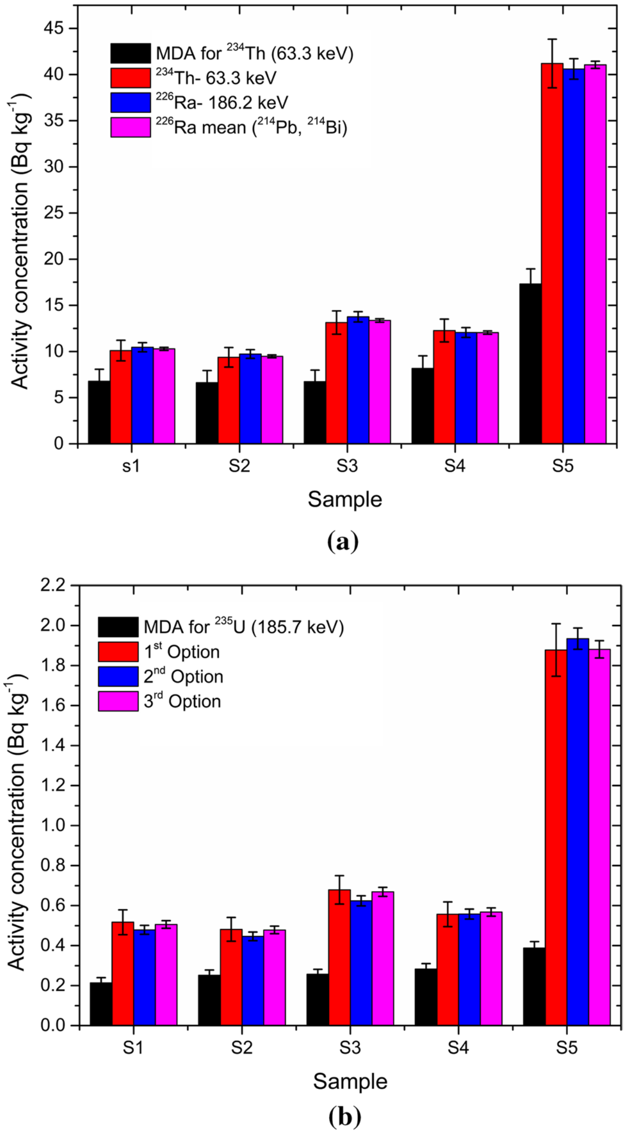

(a)

(b)

Fig. 6 The activity concentrations of ^{234}Th (**a**) and ^{235}U (**b**) for the rock samples

Conclusions

This study has described a rapid and reliable analytical procedure to determine the radioactivities in cylindrical solid samples using gamma spectrometry in detail. The self-absorption and the coincidence summing factors which were calculated by using the MCNP-CP code were also considered in the measurements. The ^{238}U activity concentration was determined according to the measurement of ^{234}Th (63.3 keV) taking into account the self-absorption correction factor and the contribution count of ^{232}Th (63.8 keV). The measurement of ^{235}U activity will be obtained from the new analytical procedure regardless of the secular equilibrium of ^{226}Ra—its daughters (^{214}Pb and ^{214}Bi) as well as the natural ratio of ^{235}U–^{238}U. The radioactivities obtained for the CRM samples showed good agreement with the certified reference values with relative deviations of less than 3%. Moreover, the IAEA proficiency test received “Accepted” for all radionuclides analysis. This verifies that the advanced analytical procedure was simple, useful, and reliable for analytical laboratories using gamma spectrometry. This procedure can be applied immediately after the sample preparation regardless of the existence of a secular equilibrium between ^{226}Ra and its progenies (^{214}Pb, ^{214}Bi) and regardless of the existence of equilibrium between ^{238}U and ^{226}Ra or normal ^{235}U–^{238}U isotopic ratio. However, it was important for this procedure that the FEP efficiency and the self-absorption correction and the interference correction must be taken into consideration for good quality analysis.

Supplementary Information The online version contains supplementary material available at https://doi.org/10.1007/s10967-023-08773-z.

Acknowledgements The authors would like to thank Dr. Andrey Berlizov for support with the MCNP-CP code, MSc. Huynh Dinh Chuong for preparing samples, MSc. Vu Tuan Minh and MSc. Le Dinh Hung for experimental measurements required for this work. This research is funded by Vietnam National University Ho Chi Minh City (VNU-HCM) under grant number VL2021-18-01.

Declarations

Conflict of interest The authors declare that they have no conflict of interest.

References

1. Baeza A, Caballero JM, Corbacho JA, Ontalba MA, Vasco J (2020) Response of an automatic air monitoring gamma-spectrometry station based on sample retention to rainfall-caused dosimetric alterations and to environments with a wide range of radon levels. Radiat Meas 134:106324
2. Barba-Lobo A, Miguel EGS, Lozano RL, Bolívar JP (2021) A general methodology to determine natural radionuclides by well-type HPGe detectors. Measurement 181:109561
3. Corte FD, Umans H, Vandenberghe D, Wispelaere AD, Haute PDV (2005) Direct gamma-spectrometric measurement of the ^{226}Ra 186.2 keV line for detecting ^{238}U/^{226}Ra disequilibrium in determining the environmental dose rate for the luminescence dating of sediments. Appl Radiat Isot 63:589–598
4. Abdualhadi SA, Mauz B, Joss SDT, Nolan PJ (2018) Detecting and quantifying uranium-series disequilibrium in natural samples for dosimetric dating applications. Radiat Meas 114:25–31
5. Huy NQ, Hien PD, Luyen TV, Hoang DV, Hiep HT, Quang NH, Long NQ, Nhan DD, Binh NT, Hai PS, Ngo NT (2012) Natural radioactivity and external dose assessment of surface soils in Vietnam. Radiat Prot Dosim 151:522–531
6. Santos JMND, Júnior JADS, Amaral RDS, Fernández ZH, Bezerra JD, Bezerra MBCF, Silva ANCDS, Araújo EEND, Rojas LAV, Milan MO, Correia FLDB (2019) Monitoring and characterisation of new evidence of natural radionuclides in rock outcrops in PARAÍBA-BRAZIL. Radiat Prot Dosim 187:310–320
7. Ho PL, Hung LD, Minh VT, Chinh DV, Thanh TT, Tao CV (2020) Assessment of radioactivity and chemical contaminants in domestic water at supply stations in Long Phu District, Vietnam, to prevent public health risks. Sci Total Environ 737:140291
8. Gray PJ, Zhang L, Xu H, McDiarmid M, Squibb K, Centeno JA (2012) Determination of ^{236}U/^{238}U and ^{235}U/^{238}U isotope ratios in human urine by inductively coupled plasma mass spectrometry. Microchem J 105:94–100
9. El-Galy MM, Issa FA, Desouky OA, Diab HM, Khattab MR (2011) Use of alpha spectrometry for analysis of U-isotopes in some granite samples. J Radioanal Nucl Chem 288:805–811
10. Nguyen VT, Huynh NPT, Vu NB, Le CH (2021) Long-term accumulation of 226Ra in some agricultural soils based on model assessment. Agric Water Manag 243:106453
11. Forte M, Abbate G, Badalamenti P, Costantino S, Lunesu D, Rusconi R (2015) Validation of a method for measuring ^{226}Ra in drinking waters by LSC. Appl Radiat Isot 103:143–150
12. Hung NQ, Chuong HD, Vuong LQ, Thanh TT, Tao CV (2016) Intercomparison NaI(Tl) and HPGe spectrometry to studies of natural radioactivity on geological samples. J Environ Radioact 164:197–201
13. Ho PL, Hung LD, Minh VT, Chinh DV, Thanh TT, Tao CV (2018) Natural and artificial radionuclides in tea samples determined with gamma spectrometry. J Radioanal Nucl Chem 316:703–707
14. LNHB Nucléide – Laraweb (2020). http://www.nucleide.org/Laraweb/index.php. Accessed 01 April 2020
15. Murray A, Marten R, Johnston A, Martin P (1987) Analysis for naturally occuring radionuclides at environmental concentrations by gamma spectrometry. J Radioanal Nucl Chem 115:263–288
16. El-Daoushy F, Hernández F (2002) Gamma spectrometry of ^{234}Th (^{238}U) in environmental samples. Analyst 127:981–989
17. Huy NQ, Luyen TV (2004) A method to determine ^{238}U activity in environmental soil samples by using 63.3-keV-photopeak-gamma HPGe spectrometer. Appl Radiat Isot 61:1419–1424
18. Yücel H, Solmaz AN, Köse E, Bor D (2009) Spectral interference corrections for the measurement of ^{238}U in materials rich in thorium by a high resolution gamma-ray spectrometry. Appl Radiat Isot 67:2049–2056
19. Thanh TT, Loan TTH, Nhon MV (1987) Tao CV (2014) Improvement of passive shielding to reduce background components to determinate radioactivity at low energy gamma rays. Kerntechnik 79:247–252
20. Modarresi SM, Masoudi SF (2018) On the gamma spectrometry efficiency of reference materials and soil samples. J Environ Radioact 183:54–58
21. Barba-Lobo A, Mosqueda F, Bolívar JP (2021) A general function for determining mass attenuation coefficients to correct self-absorption effects in samples measured by gamma spectrometry. Radiat Phys Chem 179:109247
22. Anilkumar S, Deepa AK, Narayani K, Rekha AK, Achuthan PV, Krishnamachari G, Sharma DN (2008) Estimation of ^{235}U concentration in some depleted uranium samples by high resolution gamma-ray spectrometry using 185 keV and 1001 keV gamma-energies of ^{235}U and ^{234m}Pa. J Radioanal Nucl Chem 274:161
23. Ebaid YY, El-Mongy SA, Allam KA (2005) ^{235}U–γ emission contribution to the 186 keV energy transition of ^{226}Ra in environmental samples activity calculations. Int Congr Ser 1276:409–411
24. Völgyesi P, Kis Z, Szabó Z, Szabó C (2014) Using the 186-keV peak for ^{226}Ra activity concentration determination in Hungarian coal-slag samples by gamma-ray spectroscopy. J Radioanal Nucl Chem 302:375–383
25. Vuong LQ, Chuong HD, Nguyen VH, Hung NQ, Thanh TT, Tao CV (2017) Revision of nuclear data of ^{235}U and ^{226}Ra for the 186-keV gamma-ray peak for the determination of activity in environmental samples. J Radioanal Nucl Chem 314:1273–1277
26. Al-Masri MS, Hasan M, Al-Khateeb Y (2020) Preparation of produced water reference material for analyzing ^{226}Ra by gamma spectrometry. J Radioanal Nucl Chem 324:225–231
27. Ramebäck H, Lagerkvist P, Holmgren S, Jonsson S, Sandström B, Tovedal A, Vesterlund A, Vidmar T, Kastlander J (2016) On the accuracy of gamma spectrometric isotope ratio measurements of uranium. Nucl Instrum Methods Phys Res Sect A 815:57–61
28. Berlizov AN (2012) MCNP-CP Upgrade patch version 3.2: a correclated particle source extension of a general purpose Monte Carlo N-particle transport code. Institute for Nuclear Research National Academy of Sciences of Ukraine
29. Thanh TT, Ferreux L, Lépy MC, Tao CV (2010) Determination activity of radionuclides in marine sediment by gamma spectrometer with anti cosmic shielding. J Environ Radioact 101:780–783
30. NIST XCOM: Photon cross sections database. https://physics.nist.gov/PhysRefData/Xcom/html/xcom1.html. Accessed 01 April 2020
31. Huy NQ, Binh DQ, An VX, Loan TT, Can NT (2013) Self-absorption correction in determining the ^{238}U activity of soil samples via 63.3 keV gamma ray using MCNP5 code. Appl Radiat Isot 71:11–20

32. Thanh TT, Vuong LQ, Ho PL, Chuong HD, Nguyen VH, Tao CV (2018) Validation of an advanced analytical procedure applied to the measurement of environmental radioactivity. J Environ Radioact 184–185:109–113
33. Maestro-32 (2003) Software User's Manual Vesion 6. ORTEC, Advanced Measurement Technology, Inc., U.S.A
34. Lépy MC (2004) Presentation of the COLEGRAM software. Note tech LNHB 04/26
35. Bruker X-ray Fluorescence Model S2. https://www.bruker.com/en/products-and-solutions/elemental-analyzers/xrf-spectrometers/s2-puma-series2.html. Accessed 01 April 2020
36. Done L, Ioan MR (2016) Minimum detectable activity in gamma spectrometry and its use in low level activity measurements. Appl Radiat Isot 114:28–32
37. Sima O, Ott ADVO, Dias MS, Dryak P, Ferreux L, Gurau D, Hurtado S, Jodlowski P, Karfopoulos K, Koskinas MF, Laubenstein M, Lee YK, Lépy MC, Luca A, Menezes MO, Moreira DS, Nikolič J, Peyres V, Saganowski P, Savva MI, Semmler R, Solc J, Thanh TT, Tyminska K, Tyminski Z, Vidmar T, Vukanac I, Yucel H (2020) Consistency test of coincidence-summing calculation methods for extended sources. Appl Radiat Isot 155:108921
38. Ordóñez J, Gallardo S, Ortiz J, Martorell S (2019) Coincidence summing correction factors for ^{238}U and ^{232}Th decay series using the Monte Carlo method. Radiat Phys Chem 155:244–247
39. Vargas MJ, Timón AF, Díaz NC, Sánchez DP (2002) Monte Carlo simulation of the self-absorption corrections for natural samples in gamma-ray spectrometry. Appl Radiat Isot 57:893–898
40. GUM (2008) Evaluation of measurement data—guide to the expression of uncertainty in measurement. JCGM 100:2008
41. Ji Y-Y, Lim J-M, Kim H, Kim C-J, Lim C-S, Chung KH (2017) Limitations of gamma-ray spectrometry in the quantification of ^{238}U and ^{232}Th in raw materials and by-products. J Radioanal Nucl Chem 311:1163–1168
42. Lépy C, Ferreuz L, Hamon C, Plagnard J (2008) Logicised d'ajustement des courbes de rendement ACORES. Note technique LNHB 2008–2045
43. ISO GUIDE 35:2017 (2017) Reference materials - Guidance for characterization and assessment of homogeneity and stability. International Organization for Standardization, Switzerland
44. Abdellah W (2019) Determination of Radium-226 in rock samples by liquid scintillation counter. Open J Appl Sci 09:270–284
45. Bojanowski R, Radecki Z, Piekoś R (2002) Rapid determination of 226Ra and uranium isotopes in solid samples by fusion with lithium metaborate and alpha spectrometry. Sci World J 2:1891–1905
46. Osvath I, Tarjan S, Pitois A, Groening M, Osborn D (2016) IAEA's ALMERA network: supporting the quality of environmental radioactivity measurements. Appl Radiat Isot 109:90–95
47. Lu X, Zhang X (2008) Natural radioactivity measurements in rock samples of Cuihua mountain national geological park, China. Radiat Prot Dosim 128:77–82
48. Al-Trabulsy HA, Khater AEM, Habbani FI (2011) Radioactivity levels and radiological hazard indices at the Saudi coastline of the Gulf of Aqaba. Radiat Phys Chem 80:343–348
49. Harb S, Abbady AE-B, El-Kamel AE-H, Saleh II, Abd El-Mageed AI (2012) Natural radioactivity and their radiological effects for different types of rocks from Egypt. Radiat Phys Chem 81:221–225
50. Rangaswamy DR, Srilatha MC, Ningappa C, Srinivasa E, Sannappa J (2016) Measurement of natural radioactivity and radiation hazards assessment in rock samples of Ramanagara and Tumkur districts, Karnataka, India. Environ Earth Sci 75:373
51. Dżaluk A, Malczewski D, Żaba J, Dziurowicz M (2018) Natural radioactivity in granites and gneisses of the Opava Mountains (Poland): a comparison between laboratory and in situ measurements. J Radioanal Nucl Chem 316:101–109
52. Birami FA, Moore F, Faghihi R, Keshavarzi B (2019) Distribution of natural radionuclides and assessment of the associated radiological hazards in the rock and soil samples from a high-level natural radiation area, Northern Iran. J Radioanal Nucl Chem 322:2091–2103
53. Box G, Hunter S, Hunter W (2005) Statistics for experimenters. Design, innovation, and discovery. 2nd ed, vol 2. John Wiley & Sons INC, Publication
54. Vesterbacka P, Klemola S, Salahel-Din K, Saman M (2009) Comparison of analytical methods used to determine ^{235}U, ^{238}U and ^{210}Pb from sediment samples by alpha, beta and gamma spectrometry. J Radioanal Nucl Chem 281:441–448
55. Giubrone G, Ortiz J, Gallardo S, Martorell S, Bas MC (2016) Calculation of coincidence summing correction factors for an HPGe detector using GEANT4. J Environ Radioact 158–159:114–118
56. Mahmoud RK (2021) Uranium-series disequilibrium as a tool for tracing uranium accumulation zone in altered granite rocks. Int J Environ Anal Chem 101:1750–1760